Taylor & Francis
Taylor & Francis Group

Simulation research of TEG-ORC combined cycle for cascade recovery of vessel waste heat

Changxin Liu, Huaan Li, Wenxiang Ye, Jianhao Liu, Huibin Wang, Minyi Xu, Xinxiang Pan, Zhuofan Mao & Shuojia Yang

Published online: 18 Apr 2021.

Submit your article to this journal ⎘

Article views: 20

View related articles ⎘

View Crossmark data ⎘

Taylor & Francis
Taylor & Francis Group

Check for updates

Simulation research of TEG-ORC combined cycle for cascade recovery of vessel waste heat

Changxin Liu [a], Huaan Li [a], Wenxiang Ye [a], Jianhao Liu [a], Huibin Wang[b], Minyi Xu [a], Xinxiang Pan[c], Zhuofan Mao [a], and Shuojia Yang[a]

aCollege of Marine Engineering, Dalian Maritime University, Dalian, China; bChina Classification Society Zhoushan Office, Zhoushan, China; cMaritime College, Guangdong Ocean University, Zhanjiang, China

ABSTRACT

The waste heat of ships has the characteristics of large temperature gradient, huge recoverable amount and various properties. Traditional technologies such as thermoelectric power generation (TEG) and organic Rankine cycle (ORC) are difficult to take into account the different characteristics of the various types of waste heat from ships. In order to realize the efficient cascade utilization of various waste heat from ships, improve the efficiency and meet the stringent requirements of the new international carbon emission regulations, a cascade recovery system of ship waste heat based on TEG-ORC (thermoelectric power generation/organic Rankine cycle) is proposed in this paper. After designing of the TEG-ORC combined cycle experimental system, the simulation research has also been carried out. The effects of TEG bottom cycle scale, ORC working medium flow rate and evaporation pressure on system net output power, system power generation cost and bottom cycle ratio (Q_{TEG}/Q_{ORC}) are studied. The results show that the TEG-ORC combined cycle overcomes the limitation of single waste heat utilization method, realizes multi-stage utilization of ship waste heat, as well as improves the utilization of waste heat. Of course, the stability and safety of ORC bottom cycle operation are also promoted. The simulation results show that when the TEG bottom cycle scale is 22 pieces, ORC working medium flow rate is 0.44 kg/s, and ORC working medium evaporation pressure is 2.2MPa, the system economy is optimal. At this time, the system power generation cost is 0.26 \$/kW·h, the system net output power is 2520.3 W, and the thermal efficiency is 23.33%.

1. Introduction

Transportation industry plays an important role in modern economic development and industrial production. It is also a key industry that consumes energy and causes environmental pollution. The proportion of CO_2 produced by transportation industry in the whole industry is as high as 23%. As one of the cheapest ways of transportation, ship has the advantages of low freight rate, suitable for long distance and large amount transportation. It also plays an extremely important role in the development of our world economy. The maritime industry carries more than 90% of the world's commodity trade freight amount. As the main carrier of the maritime industry, there are large energy consumption and serious waste heat waste (Cai et al., 2010). According to statistics, the proportion of energy consumption in the total operating cost of ships is about 25–30% for small transport vessels, 35% for regular passenger and cargo ships, 50% for bulk carriers and 60% for oil tankers (Mei 2011).

At present, many researchers have carried out effective research on ship waste heat recovery by means of thermoelectric power generation (TEG) and organic Rankine cycle (ORC). Yan evaluated the performance of TEG for the recovery of vehicle exhaust heat, and verified its feasibility (Liu 2013; Liu and Li 2014, 2015; Zhang et al. 2014, 2014b; Wang et al. 2016). Song conducted a study on the recovery of waste heat from marine main engine flue gas and cylinder liner water based on ORC (Song, Song, and Gu 2015). The results show that when R245fa and benzene are employed as working mediums, the total output power of the two systems is about 101.1 kw, and the efficiency of the main engine is increased by 10.2%. Girgini carried out thermodynamic modeling and analysis on the application of ORC system in the recovery of flue gas waste heat of marine power generation diesel engine. Among the seven refrigerants, toluene shows the best performance and the system efficiency reaches 32% (Girgin et al. 2017). Miller was the first to propose a system combining TEG and ORC, and to carry out theoretical research. High temperature flue gas can pass through TEG unit, make temperature drop while generating electricity, and then enter evaporator to preheat ORC working medium, so as to realize safe and efficient utilization of the high temperature waste heat (Miller, Hendricks, and Peterson 2009; Miller et al. 2011). Shu designed a system combining TEG and ORC for vehicle waste heat recovery with R123 as working medium (Shu et al. 2012a, 2012b). The simulation results show that under the optimal working conditions, the TEG-ORC combined cycle system has an evaporation pressure of 4MPa and a condensation pressure of 0.06 MPa. Under this condition, the output power of the system is 27.68 kw, and the system efficiency can reach 45.00%.

Through the previous research on waste heat utilization by TEG and ORC, in this paper, a new cascade utilization method of ship waste heat based on TEG-ORC combined cycle is proposed (Liu et al. 2019, 2020, 2017; Wang et al. 2018). Theoretical model of TEG-ORC combined cycle is established, and experimental system is designed. In this article, according to the main engine flue gas, the ratio of TEG bottom cycle and ORC bottom cycle to the waste heat utilization is defined as Q_{TEG}/Q_{ORC}. To find out the coupling characteristics of each bottom cycle in the combined cycle, the relationship among ORC working medium evaporation pressure (p), ORC working medium flow rate (m_{ORC}), TEG bottom cycle scale (N_{TEG}) and system net output power (W_{net}), bottom cycle ratio (Q_{TEG}/Q_{ORC}), system power generation cost (C_g) was studied by simulation methods.

2. System designed

Although the thermal efficiency of TEG bottom cycle($\eta 1$) is low, it can realize the recovery of high temperature waste heat with low cost. ORC technology can realize the recovery of medium and low temperature waste heat with relatively high efficiency, but its size is large and C_g is relatively high. The waste heat of ships has the characteristics of large temperature gradient, huge recoverable amount and various properties. It is difficult to recover from various ship waste heat by single technology. The main types and characteristics of waste heat are shown in Table 1, and the TEG-ORC combined cycle experimental system is presented in Figure 1. Q_C – Heat absorbed power of the cold end of the TEG unit, (in W). Q_H

– The release power of the hot end of the TEG unit, (in W). Q_2 – Heat absorption power of working medium in secondary preheater, (in W). Q_3 – Heat absorption power of working medium in third-stage preheater, (in W). Q_{eva} – Heat absorption power of working medium in evaporator, (in W). Q_{ORC} – ORC bottom cycle output power, (in W).h_2 – The enthalpy of the working medium before and after preheating by the working medium pump, (in kJ/kg). h_3 – The enthalpy of the working medium after preheating at the cold end of the TEG bottom cycle, (in kJ/kg). h_4 – The enthalpy of the working medium after being preheated by the secondary preheater, (in kJ/kg). h_5 – The enthalpy of the working medium after being preheated by the third-stage preheater, (in kJ/kg). h_6 – Enthalpy of saturated vapor, (in kJ/kg). h_7 – Enthalpy of exhaust steam after expansion, (in kJ/kg). W_{TEG} – Output power of TEG system, (in W).W_{exp} – Output power of expander, (in W). m – Working medium flow, (in kg/s).

In TEG bottom cycle, in order to overcome the heat transfer bottleneck at the cold and hot ends of TEG unit, a heat pipe was designed to enhance heat transfer. When the flue gas of the main engine flows through the TEG unit, the waste heat reaches the evaporation section of the heat pipe and the heat is transferred to the condensing section after the phase change heat transfer of the working medium. The condensation section is the hot end of the TEG unit, it realizes the first utilization of flue gas waste heat. Organic working medium is employed as cold source while TEG is realized and the first-stage preheating of ORC working medium is also finished with the help of flue gas waste heat. The flue gas temperature is reduced, which ensures the safety of

Table 1. Types and characteristics of ship waste heat.

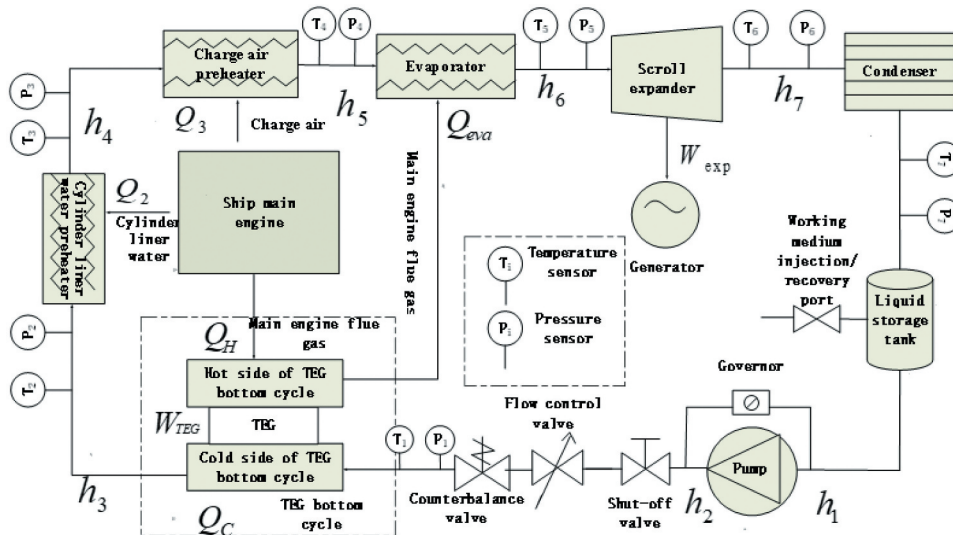| Ship waste heat	Temperature range of waste heat (K)	Characteristics of waste heat
Waste heat of flue gas from marine main engine	523 ~ 573	Large amount, high temperature waste heat
Waste heat of cylinder liner water	About 358	Large amount, low temperature waste heat
waste heat of charge air	About 423	Large amount, medium temperature waste heat

Figure 1. Experimental system of TEG-ORC combined cycle.

ORC bottom cycle waste heat utilization. In the ORC bottom cycle, after the organic working medium has achieved the first-stage preheating at the cold end of the TEG unit, the secondary preheating is realized by using the waste heat of the cylinder liner water of the main engine. Then, it enters the charge air heat exchanger to realize the third-stage pre-heating while reducing the temperature of the charge air. The residual heat of the flue gas makes the organic working medium reach the optimal temperature at the evaporator outlet, so as to maximize the output power. The exhaust vapor after working reaches the condenser, the organic

working medium is cooled into liquid and then returned to the cold end of TEG unit as the cooling medium to complete the cycle.

3. Theoretical model

3.1. Thermodynamic model of TEG-ORC combined cycle

According to the principle of Seebeck effect, the heat released from the cold end of the TEG and absorbed by the hot end can be expressed as follows:
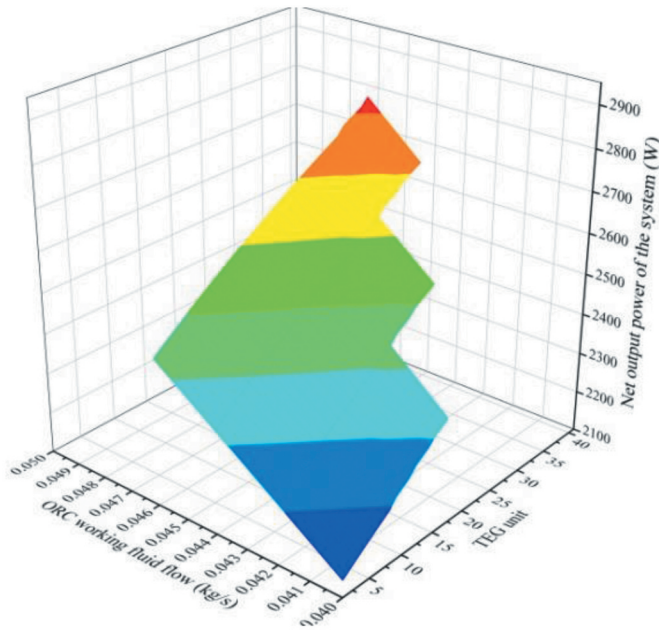
Figure 2. The variation of net output power of the system with ORC working medium flow and TEG unit.

Figure 4. The variation of net output power of the system with ORC evaporation pressure and ORC working medium flow.
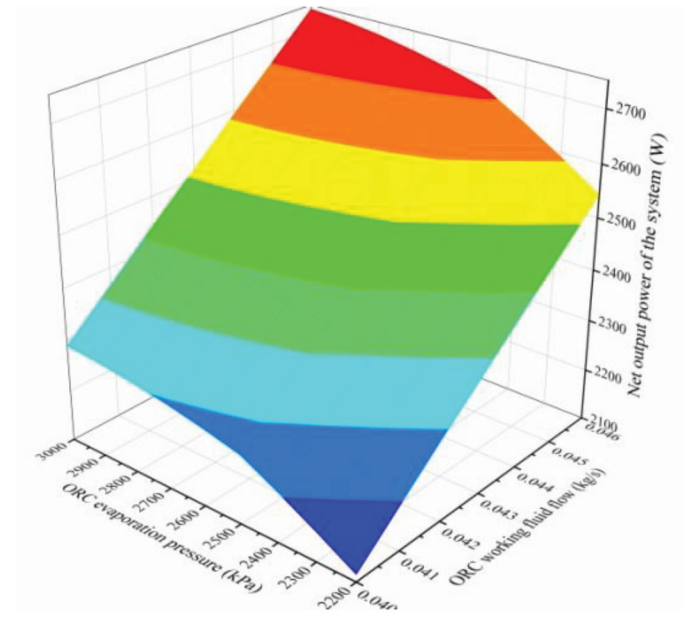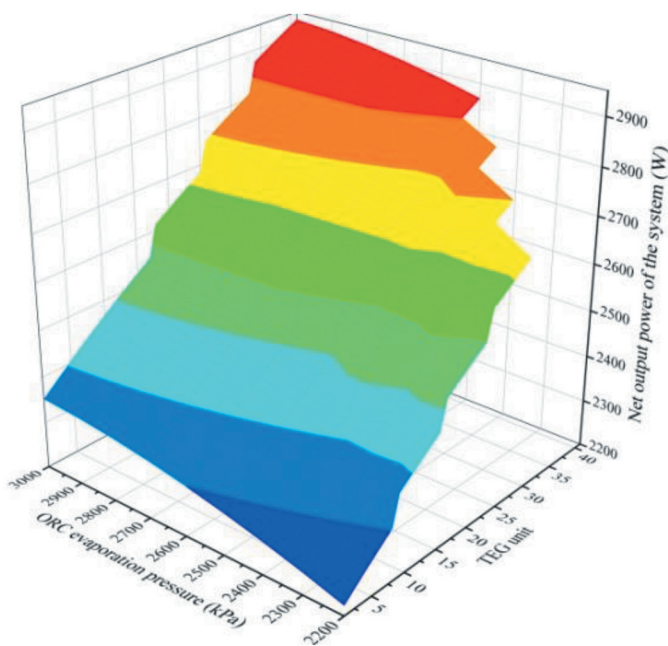

Figure 3. The variation of net output power of the system with ORC evaporation pressure and TEG unit.
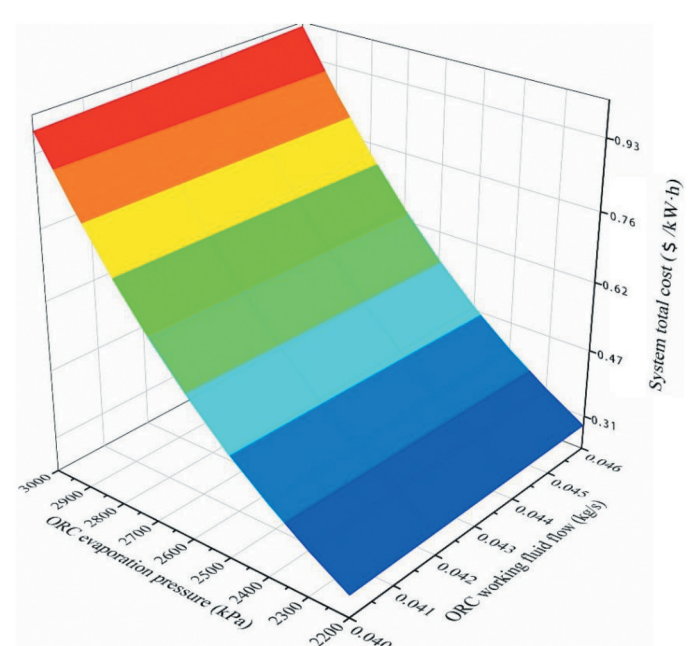

Figure 5. The variation of system total cost with ORC evaporation pressure and ORC working medium flow.
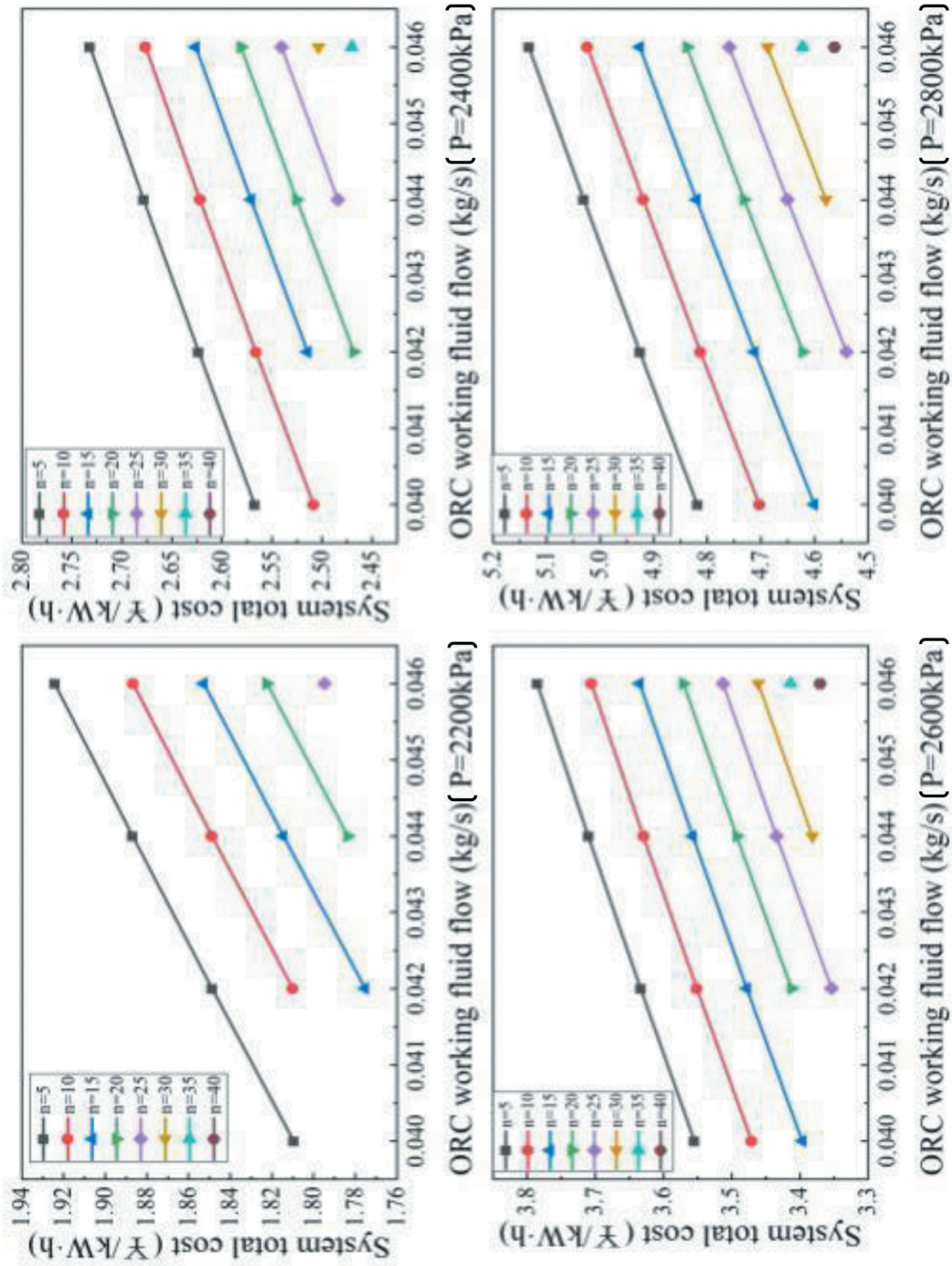
Figure 6. The variation of system total cost with ORC working medium flow under different evaporation pressure.

$$Q_C = nq_C = n[\alpha_{PN}IT_{ORC} + K_{PN}(T_H - T_{ORC}) + 0.5I^2R_{IN}] \quad (1)$$

$$Q_H = nq_H = n[\alpha_{PN}IT_H + K_{PN}(T_H - T_{ORC}) - 0.5I^2R_{IN}] \quad (2)$$

Where, n is the logarithm of P&N, (in pair). q_c is the rate of heat release by a pair of P&N junctions in unit time, (in W). q_H is the rate of heat absorption by a pair of P&N junctions in unit time, (in W). T_{ORC} is the temperature of ORC working medium, (in K). T_H is the temperature of hot end of TEG unit, (in K). K_{PN} is the thermal conductivity of P & n junction, (in W/(m·K)). R_{IN} is the resistance of a pair of P & n junction, (in Ω). I is loop current, (in A). Neglecting heat loss, the output power and conversion efficiency of the TEG system are expressed as follows:

$$W_{TEG} = Q_H - Q_C \quad (3)$$

$$\eta = 1 - Q_C/Q_H \quad (4)$$

(1) Working medium pump:
   The output power of working medium pump (*Ppump*) can be expressed as:

$$Ppump = m(h2 - h1) \quad (5)$$

(2) Flue gas preheater

The ORC working medium is preheated for the first time at the cold end of TEG unit, the heat absorption can be expressed as:

$$Q_C = Q_{TEG} = m(h_3 - h_2) \quad (6)$$

(3) Secondary preheater (cylinder liner water waste heat)

The ORC working medium is preheated by the cylinder liner water of the main engine in the secondary preheater, and its heat absorption rate can be expressed as:

$$Q_2 = m(h_4 - h_3) \quad (7)$$

(4) The third-stage preheater (charge air preheater)
   The ORC working medium is preheated by charge air in the third-stage preheater, and its heat absorption rate can be expressed as:

$$Q_3 = m(h_5 - h_4) \quad (8)$$

(5) Evaporator
   In the evaporator, ORC working medium first absorbs heat at a constant pressure to become saturated liquid, and then continues to absorb heat at constant temperature to become saturated gas state, its heat absorption rate can be expressed as:

$$Q_{eva} = Q_{ORC} = m(h_6 - h_5) \quad (9)$$

(6) Expander
   The ORC working medium steam produces work by expansion in the expander, and the corresponding output power of the expander can be expressed as:

$$W_{exp} = m(h_6 - h_7) \quad (10)$$

(7) Condenser. The exhaust steam is recondensed into saturated liquid in the condenser, and its heat release rate in the condenser can be expressed as:

$$Q_{cond} = m(h_7 - h_1) \quad (11)$$

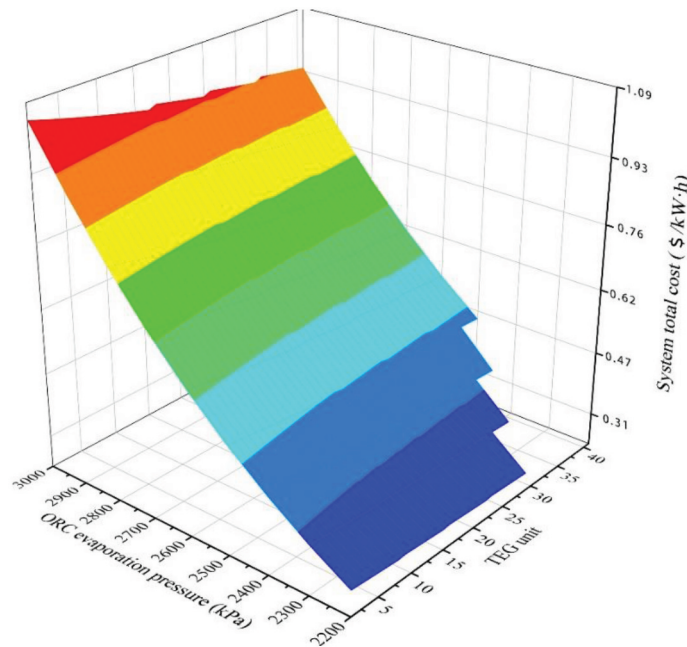Therefore, the net output power of ORC system can be expressed as:

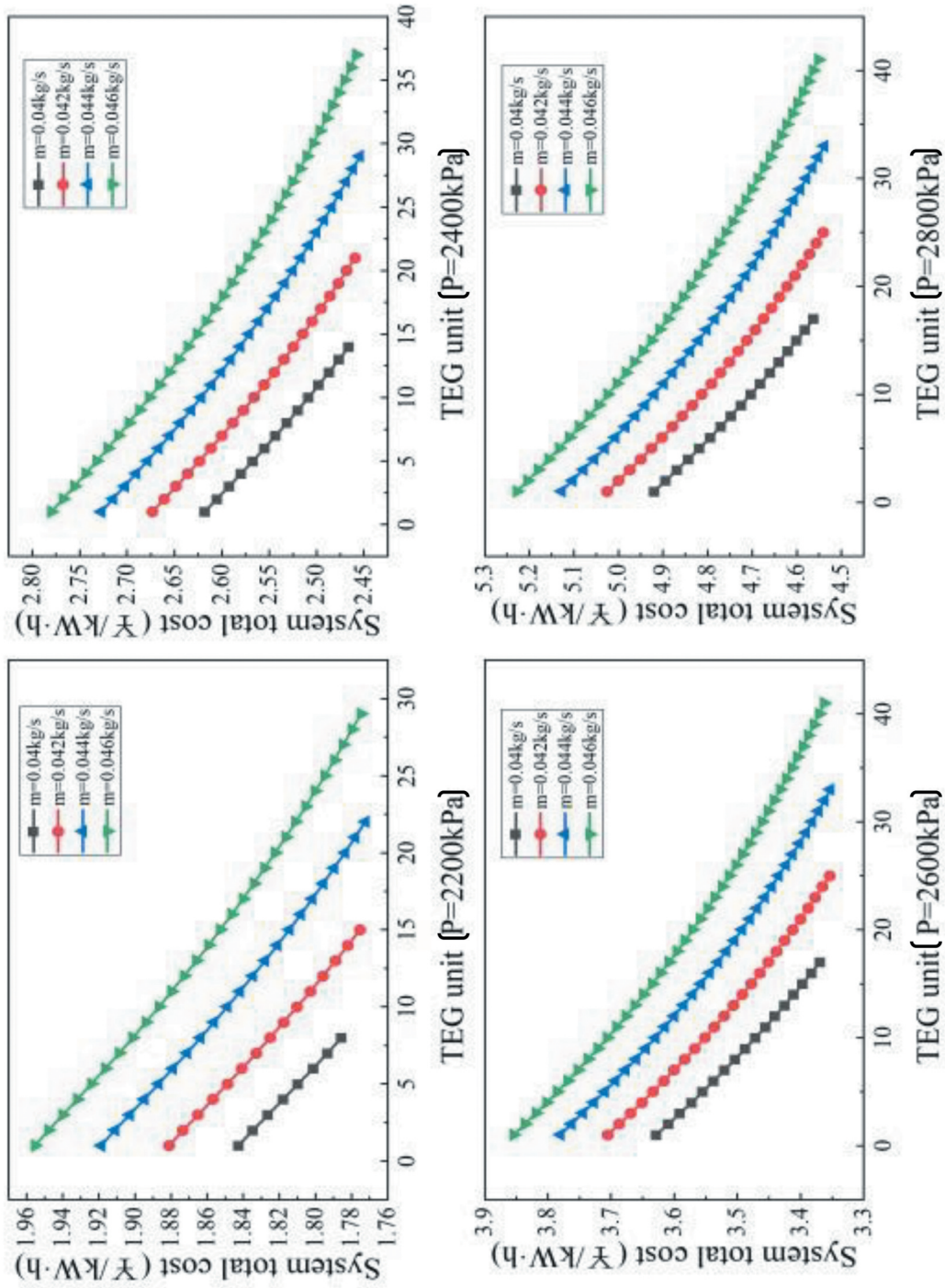**Figure 7.** The variation of system total cost with ORC evaporation pressure and TEG unit.

Figure 8. The variation of system total cost with TEG unit under different evaporation pressure.

$$C_{BM} = C_p(B_1 + B_2 F_M F_p) \qquad (18)$$

where, Cp is the basic cost of the equipment, (in dollar). Z is the dimension parameter representing the weight of the exchanger. Here, it refers to the total heat exchange of the preheater. CBM is the correction cost of equipment considering the construction material and the operating pressure. The pressure correction factor can be calculated by the following formula:

$$\lg F_p = C_1 + C_2 \lg P + C_3 (\lg P)^2 \qquad (19)$$

among them, $K1$, $K2$, $K3$, $B1$, $B2$, FM and FP are cost correction factors, and their values are shown in the Appendix A. p is the evaporation pressure, (in kPa). The equipment investment cost can be expressed as:

$$C_{BM,2019} = C_{BM,1996} \cdot CEPCI_{2019}/CEPCI_{1996} \qquad (20)$$

$$Cost_{2019} = C_{BM,2019,2} + C_{BM,2019,3} + C_{BM,2019,eva} + C_{BM,2019,exp}$$
$$+ C_{BM,2019,cond} + C_{BM,2019,pump}$$

Where, $CEPCI$ (chemical engineering plant cost index) is the cost index, $CEPCI_{1996} = 382$, $CEPCI_{2019} = 652.9$.

Concerning the cost of TEG, there is no very applicable economic model at present. Meanwhile, considering the relatively low cost of TEG and the demand for later maintenance, only the cost of pipeline devices and thermoelectric modules (TE modules) is considered in the calculation. Then, the thermal economy model of TEG is expressed as:

$$EPC\_TEG = (Cost_{pipe} + Cost_{TEM})/(W_{TEG}t_{op}) \qquad (22)$$

where, EPC_TEG is the power generation cost per kilowatt hour of TEG device, (in \$/kW·h). $Cost_{pipe}$ is the total cost of flue gas pipeline devices, (in dollar). $Cost_{TEM}$ is the total cost of installed TEG, (in dollar). W_{TEG} is the total output power of TEG, (in W).

When calculating the cost of flue gas pipeline, it is also approximately regarded as a part of the bottom cycle for heat exchange. In particular, the cost of flue gas pipeline is calculated by the same method with the ORC preheater, and it is obtained as:

$$Cost_{pipe} = C_{BM,2019} \qquad (23)$$

The cost of TEG is calculated as follows:

$$Cost_{TEM} = N \times \cos t_{TEG} \qquad (24)$$

where, N is the number of TEG, (in pair). $Cost_{TEG}$ is the unit price of TEG, (in dollar).
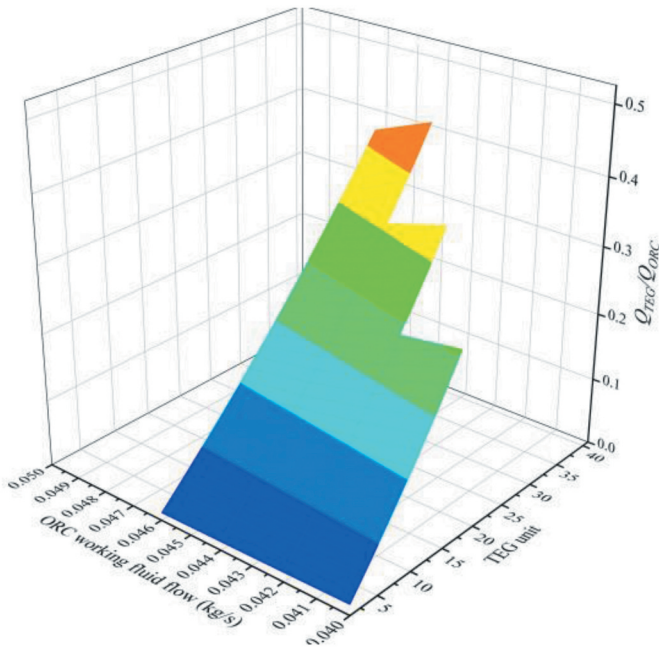

Figure 9. The variation of bottom cycle ratio with ORC evaporation pressure and ORC working medium flow.

$$W_{ORC} = W_{exp} - W_{pump} \qquad (12)$$

The total output power of TEG-ORC combined cycle system due to waste heat utilization:

$$W_{net} = W_{TEG} + W_{ORC} \qquad (13)$$

The thermal efficiency of TEG-ORC combined cycle system is expressed as:

$$\eta_t = \frac{W_{net}}{Q_{TEG} + Q_{ORC} + Q_2 + Q_3} \qquad (14)$$

3.2 Thermal economic model of TEG-ORC combined cycle

The electricity production cost (EPC) of an ORC unit in TEG-ORC combined cycle can be calculated as follows (Li 2017; Quoilin et al. 2011; Zhang, Wang, and Gao 2011):

$$EPC = (Cost_{2019} \cdot CRF + COM_{pl})/(W_{net}t_{op}) \qquad (15)$$

$$CRF = z(1+z)^{LT_{pl}}/[(1+z)^{LT_{pl}} - 1] \qquad (16)$$

where, $Cost_{2019}$ is the investment cost of system equipment, (in dollar). CRF (capital recovery factor) is the fund recovery coefficient, (in dollar). COM_{pl} is the system operation and maintenance cost, (in dollar). t_{op} is the system annual operation hours, (in h). Z is the loan annual interest rate. LT_{pl} is the system operation life, (in year).

The equipment investment cost mainly refers to the secondary preheater, the third-stage preheater, evaporator, expander, condenser and pump. The cost of each equipment is calculated by the following formulas:

$$\lg C_p = K_1 + K_2 \lg Z + K_3 (\lg Z)^2 \qquad (17)$$

4. System simulation

Targeting W_{net}, C_g and Q_{TEG}/Q_{ORC} in the TEG-ORC combined cycle system, the effects of TEG bottom cycle scale (N_{TEG}), m_{ORC} and p on the system performance are studied through system simulation. Among them, the variation range of p is from 2.2 to 3 Mpa, and the step size is 0.1 MPa. The variation range of m_{ORC} is from 0.04 to 0.05 kg/s, and the length is 0.002 kg/s. While N_{TEG} is changed by the number of TE modules, the number of TE modules is from 1 to 60 and the step size is 1
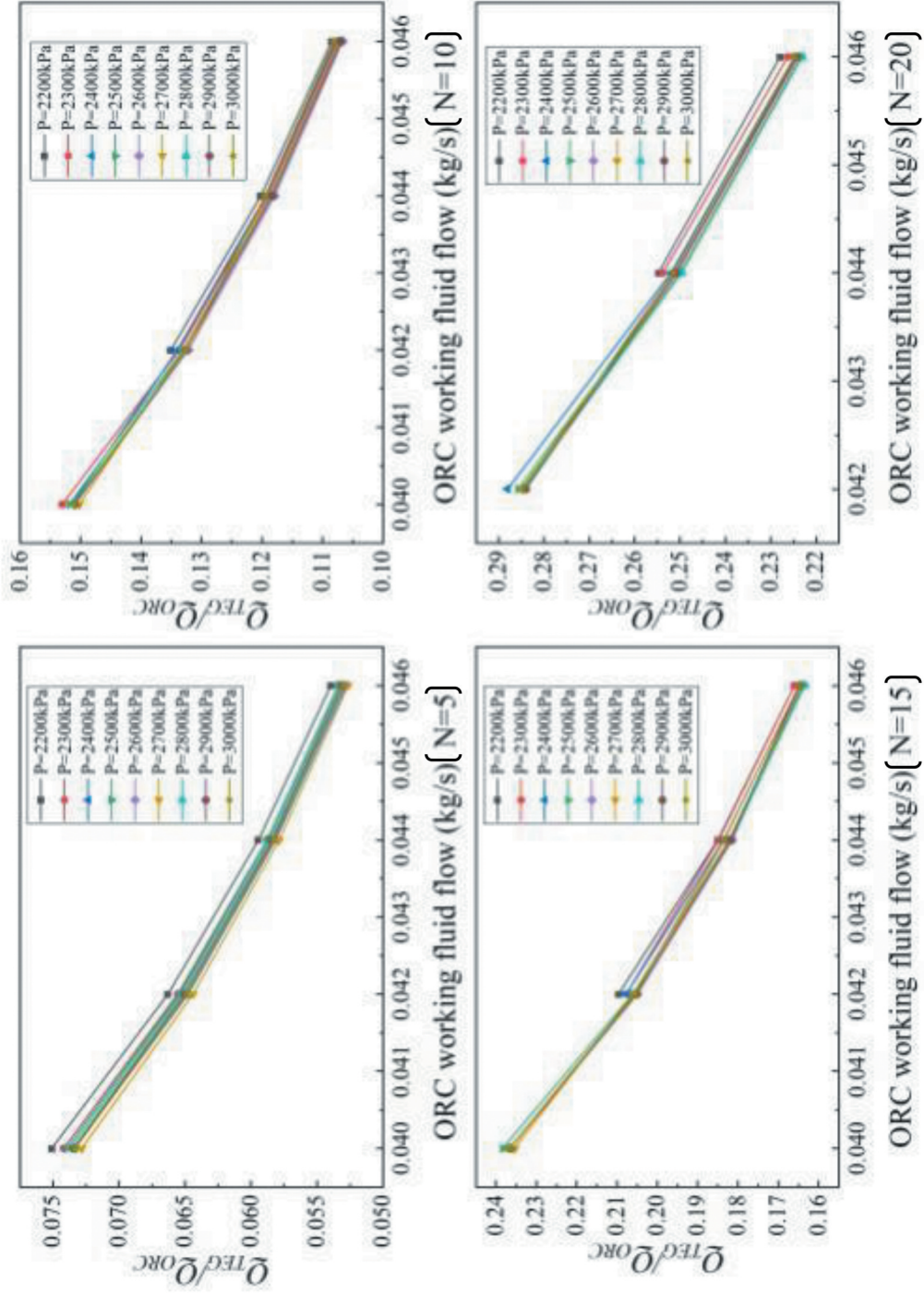
Figure 10. The variation of bottom cycle ratio with ORC working medium flow under different TEG unit.
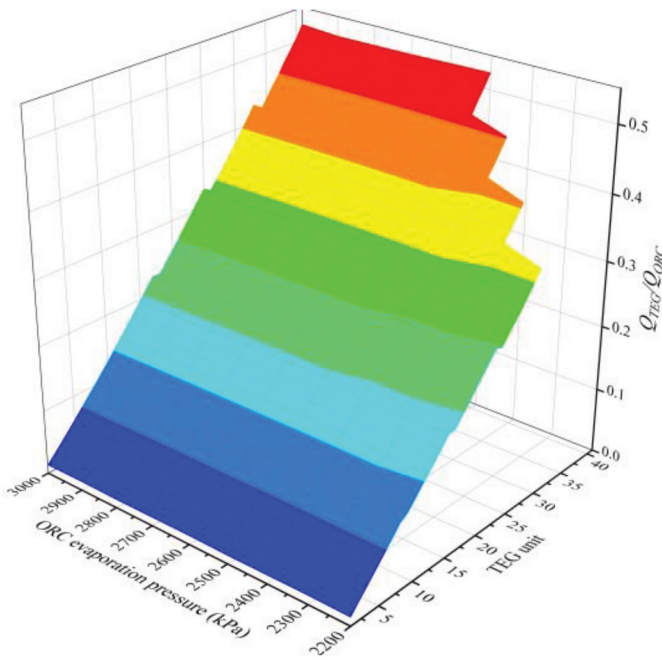
Figure 11. The variation of Q_{TEG}/Q_{ORC} with ORC evaporation pressure and TEG unit.

influence of m_{ORC} and N_{TEG} on W_{net} is obvious, and N_{TEG} has a greater impact on W_{net}. The variation of W_{net} with p and N_{TEG} is shown in Figure 3. It can be seen from Figure 3 that when p is constant, W_{net} will increase with the increase of N_{TEG}. When N_{TEG} is constant, N_{TEG} does not increase significantly with the increase of p. Therefore, in the experimental system designed in this study, the N_{TEG} has a greater effect on W_{net} than p.

W_{net} varies with p and m_{ORC} is shown in Figure 4. The simulation results show that when p is constant, the increase of m_{ORC} causes a rapid raising of W_{net}. When the m_{ORC} is constant, W_{net} also increases with the increase of p. When p reaches about 2.5MPa, the growth rate of W_{net} begins to slow down significantly.

In a certain range, W_{net} is directly proportional to m_{ORC}, p and N_{TEG}. The order of influence degree from largest to smallest is N_{TEG}, m_{ORC}, p. When p exceeds 2.5MPa, W_{net} becomes slow with the increase of p.

According to the simulation results, the maximum net output power of system (P_{max}) can reach 2933.7 W. At this moment, N_{TEG} is 41 pieces, m_{ORC} is 0.046 kg/s, p is 3Mpa, and Q_{TEG}/Q_{ORC} is 0.52. When N_{TEG} is 1 piece, m_{ORC} is 0.04 kg/s, p is 2.2 MPa, Q_{TEG}/Q_{ORC} is 0.015, the minimum system output power of system (P_{min}) is 2067.9 W.

piece. In the simulation, R245fa was employed as the ORC working medium. The flue gas temperature was set at 573 K and its flow rate was 0.05 kg/s based on the data conversion of the real ship.

4.1. System net output power analysis

Figure 2 shows the curve of W_{net} with m_{ORC} and N_{TEG}. As shown in Figure 2, when the m_{ORC} is constant, W_{net} increases with the increase of N_{TEG}. Combined with the simulation data, the

4.2. System generation cost analysis

The variation of C_g with p and m_{ORC} is shown in Figure 5. When the m_{ORC} is constant, C_g increases rapidly with the increase of p, and reaches the maximum value when p is 3Mpa. When p is constant, it can be seen from Figure 6 that C_g increases slightly with the increase of m_{ORC}. Compared with m_{ORC}, the effect of p on C_g was more significant.

Figure 7 reveals the influence of C_g with p and N_{TEG}. It can be seen from the figure that when N_{TEG} is constant, with the increase of p, C_g increases rapidly. When N_{TEG} increases,
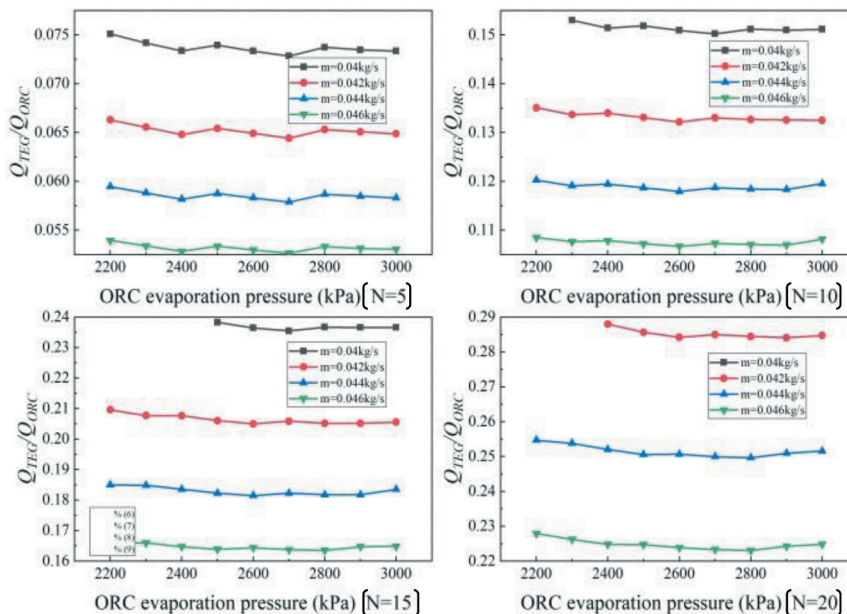

Figure 12. The variation of bottom cycle ratio with ORC evaporation pressure under different TEG unit.

C_g increases slightly with the increase of N_{TEG}. Figure 8 shows the variation curve of C_g with N_{TEG} under different p conditions. It can be seen from Figure 8 that with the increase of N_{TEG}, C_g presents a downward trend. Combined with the simulation data, it can be seen that with the increase of p, the N_{TEG} getting larger and the reduction range of C_g is getting larger. This shows that the greater the p, the greater the impact of N_{TEG} on C_g. C_g of the system increases rapidly with the increase of p, and slightly increases with the increase of m_{ORC}, but it is inversely proportional to the scale of N_{TEG}.

In the experimental system, when the N_{TEG} is 22 pieces, m_{ORC} is 0.44 kg/s, p is 2.2MPa, W_{net} is 2520.3 W, and Q_{TEG}/Q_{ORC} is 0.29, C_g is the lowest, which is 0.26 \$/kW·h. When N_{TEG} is only one piece, m_{ORC} is 0.046 kg/s, p is 3Mpa, W_{net} is 2599.2 W, Q_{TEG}/Q_{ORC} is 0.011, C_g is the highest, which is 1.02\$/kW·h.

4.3. Analysis of bottom cycle ratio

Figure 9 shows the variation of Q_{TEG}/Q_{ORC} with p and m_{ORC}. As shown in Figure 9, when the m_{ORC} is constant, Q_{TEG}/Q_{ORC} increases synchronously with the increase of N_{TEG}. As shown in Figure 10, under different N_{TEG}, the increase of m_{ORC} will reduce the Q_{TEG}/Q_{ORC}. Based on the simulation data, in the TEG-ORC combined cycle system, N_{TEG} has a greater impact on the Q_{TEG}/Q_{ORC} value than m_{ORC}.

Figure 11 shows the curve of Q_{TEG}/Q_{ORC} with p and N_{TEG}. As shown in Figure 11, when p is constant, Q_{TEG}/Q_{ORC} is proportional to N_{TEG}. Figure 12 shows the relationship between p and Q_{TEG}/Q_{ORC} under different N_{TEG}. It can be seen from Figure 12 that with the increase of p, Q_{TEG}/Q_{ORC} has only a small fluctuation, showing a slight downward trend. According to the simulation data, the influence of N_{TEG} on Q_{TEG}/Q_{ORC} is greater than that of p. Q_{TEG}/Q_{ORC} is proportional to the N_{TEG}. With the increase of m_{ORC}, the Q_{TEG}/Q_{ORC} decreased significantly. In terms of the impact on Q_{TEG}/Q_{ORC}, N_{TEG} is greater than m_{ORC} and p.

In this paper, the maximum Q_{TEG}/Q_{ORC} is 0.53, at this time, the N_{TEG} is 41 pieces, m_{ORC} is 0.046 kg/s, p is 2.5 MPa; the minimum value of Q_{TEG}/Q_{ORC} is 0.01, at this time, N_{TEG} is 1 piece, m_{ORC} is 0.046 kg/s, p is 2.5MPa.

5. Conclusion and prospect

In this paper, combined the characteristics of ship waste heat for large temperature gradient, huge recoverable amount and various properties, integrated the respective advantages of TEG and ORC, a theoretical model of TEG-ORC combined cycle on ship waste heat recovery system is proposed. Based on the TEG-ORC combined cycle thermodynamic model and thermal economic model, the TEG-ORC combined cycle system with R245fa as working medium was simulated and optimized. In the simulation process, with m_{ORC}, p and N_{TEG} scale as variable parameters, the performance of W_{net}, C_g and Q_{TEG}/Q_{ORC} were investigated. Through simulation, the variation law of the system important performance parameters with the variable parameters is obtained, and the optimal solution is found through screening. When N_{TEG} is 22 pieces, m_{ORC} is 0.44 kg/s, and p is 2.2 MPa, the system economy is optimal. At this moment, C_g is 0.2736 (\$/kW·h), W_{net} is 2520.3 W, and η_t is 23.33%.

ORCID

Changxin Liu http://orcid.org/0000-0002-4748-1265
Huaan Li http://orcid.org/0000-0002-4116-9983
Wenxiang Ye http://orcid.org/0000-0003-1491-3348
Jianhao Liu http://orcid.org/0000-0001-7676-7783
Minyi Xu http://orcid.org/0000-0002-3772-8340
Zhuofan Mao http://orcid.org/0000-0001-8377-1588

Data availability

The data that support the findings of this study is available from the corresponding author upon reasonable request.

References

Cai Y, Z. Liu, and E. Kobayashi. 2010. Improving concordance of expert judgment in formal safety assessment. J Jpn Marit Soc 176 (3): 50. doi:10.18949/jinnavi.176.0_50.

Girgin, I., and C. Ezgi. 2017. Design and thermodynamic and thermo-economic analysis of an organic Rankine cycle for naval surface ship applications[J]. *Energy Conversion and Management* 148 (9):623–34. doi:10.1016/j.enconman.2017.06.03.

Li, C. C. 2017. Simultaneous performance optimization of organic rankine cycle (ORC) system for recovering low temperature waste-heat from flue gas. 11-12. Chongqing, China: Chongqing University.

Liu, C. X. 2013. Experimental study of thermoelectric power generation system and its application. 38-109. Dalian, China: Dalian University of Technology.

Liu, C. X., F. M. Li, C. Zhao, W. X. Ye, K. D. Wang, and W. Y. Gao. 2019. Experimental research of thermal electric power generation from ship incinerator exhaust heat. IOP Conference Series Earth and Environmental, Sanya, China. 227: 22031. doi:10.1088/1755-1315/227/2/022031

Liu, C. X., W. X. Ye, J. H. Liu, G. P. Lv, T. Q. Zhao, and J. M. Dong. 2020. Study on TEG-ORC combined cycle performance for cascade recovery from vessel various waste heat. *Chinese Journal of Engineering*. doi:10.13374/j.2095-9389.01.23.001.

Liu, C. X., and W. Z. Li. 2014. An experimental study of a novel prototype for thermoelectric power generation from vehicle exhaust. *Distributed Generation & Alternative Energy Journal* 29 (2):8–23. doi:10.1080/21563306.2013.10750234.

Liu, C. X., and W. Z. Li. 2015. An experimental study of a two-stage thermoelectric generator using heat pipe in vehicle exhaust. *Distributed Generation & Alternative Energy Journal* 30 (1):15–37. doi:10.1080/21563306.2015.11101969.

Liu, C. X., Z. S. Zheng, Y. F. Lv, Y. X. Sui, H. B. Wang, and X. Zhang. 2017. Experimental study for vessel exhaust heat recovery based on two-stage thermoelectric generation. *Ship Engineering* 39 (1):31–34. doi:10.13788/j.cnki.cbgc.2017.01.030.

Mei, L. 2011. *Study on novel recovery system for marine diesel engine waste heat.* Wuhan: Wuhan University of Technology.

Miller, E. W., T. J. Hendricks, H. Wang, and R. B. Peterson. 2011. Integrated dual-cycle energy recovery using thermoelectric conversion and an organic Rankine bottoming cycle. *Proceedings of the Institution of Mechanical Engineers, Part A: Journal of Power and Energy* 225 (1):33–43. doi:10.1177/2041296710394238.

Miller, E. W., T. J. Hendricks, and R. B. Peterson. 2009. Modeling energy recovery using thermoelectric conversion integrated with an organic rankine bottoming cycle. *Journal of Electronic Materials* 38 (7):1206–13. doi:10.1007/s11664-009-0743-1.

Quoilin, S., D. Sébastien, B. F. Tchanche, and V. Lemort. 2011. Thermo-economic optimization of waste heat recovery organic rankine cycles. *Applied Thermal Engineering* 31 (14–15):2885–289. doi:10.1016/j.applthermaleng.2011.05.014.

Shu, G. Q., J. Zhao, H. Tian, H. Q. Wei, X. Y. Liang, G. P. Yu, and L. Liu. 2012b. Theoretical analysis of engine waste heat recovery by the combined thermo-generator and organic rankine cycle system. *SAE Tech Papers.* 107 (4):636–644.

Shu, G. Q., J. Zhao, H. Tian, X. Y. Liang, and H. Q. Wei. 2012a. Parametric and exergetic analysis of waste heat recovery system based on thermo-electric generator and organic rankine cycle utilizing R123. *Energy* 45 (1):806–16. doi:10.1016/j.energy.2012.07.010.

Song, J., Y. Song, and C. W. Gu. 2015. Thermodynamic analysis and performance optimization of an Organic Rankine Cycle (ORC) waste heat recovery system for marine diesel engines. *Energy* 82:976–85. doi:10.1016/j.energy.2015.01.108.

Wang, H. B., Z. Y. Wang, Y. F. Lv, Y. X. Sui, Z. S. Zheng, and C. X. Liu. 2018. Numerical simulation and experimental study on exhaust heat of ship diesel engine based on TEG. *Ship Engineering* 40 (2):8–11. doi:10.13788/j.cnki.cbgc.2018.02.008.

Wang, X. Z., B. Li, Y. Y. Yan, S. Liu, and J. Li. 2016. A study on heat transfer enhancement in the radial direction of gas flow for thermoelectric power generation. *Applied Thermal Engineering* 102:176–83. doi:10.1016/j.applthermaleng.2016.03.063.

Zhang, S. J., H. X. Wang, and T. Gao. 2011. Performance comparison and parametric optimization of subcritical Organic Rankine Cycle (ORC) and transcritical power cycle system for low-temperature geothermal power generation. *Applied Energy* 88 (8):2740–54. doi:10.1016/j.apenergy.2011.02.034.

Zhang, X. F., C. X. Liu, R. Boukhanouf, Y. Y. Yan, and W. Z. Li. 2014a. Experimental study of a domestic thermoelectric cogeneration system. *Applied Thermal Engineering* 62 (1):69–79. doi:10.1016/j.applthermaleng.2013.09.008.

Zhang, X. F., C. X. Liu, Y. Y. Yan, and Q. Wang. 2014b. A review of thermoelectrics research – Recent developments and potentials for sustainable and renewable energy applications. *Renewable and Sustainable Energy Reviews* 32:486–503. doi:10.1016/j.rser.2013.12.053.

Appendix A

Symbol	Representativeness	Unit
B_1, B_2	Cost correction factor	
C_{BM}	Equipment modification cost considering material and pressure	
C_p	Basic cost of equipment	dollar
COM_{pl}	System operation and maintenance cost	dollar
CRF	Fund recovery coefficient	dollar
$Cost_{2019}$	Investment cost of system equipment	dollar
$Cost_{TEM}$	Total cost of installed thermoelectric generator blades	dollar
$\cos t_{TEG}$	Unit price of thermoelectric generator	dollar
EPC_TEG	Generation cost per kilowatt hour of thermoelectric power plant	$/kW·h
N_{TEG}	TEG bottom cycle scale	
F_M	Cost correction factor	
F_p	Pressure correction factor	
h_1	Enthalpy value of working medium before boosting	kJ/(kg · K)
h_2	Enthalpy value of working medium after boosting pressure	kJ/(kg · K)
h_3	The enthalpy value of the working medium after the cold end of the thermoelectric power unit is preheated	kJ/(kg · K)
h_4	The enthalpy value of the working medium after being preheated by the secondary preheater	kJ/(kg · K)
h_5	The enthalpy value of the working medium after being preheated by the three-stage preheater	kJ/(kg · K)
h_6	Enthalpy of saturated steam	kJ/(kg · K)
h_7	Enthalpy of exhaust steam after expansion	kJ/(kg · K)
K_{PN}	P&N junction thermal conductivity	W/(m · K)
K_1, K_2, K_3	Cost correction factor	
LT_{pl}	System operating life	year
m	Working medium flow	kg/s
$mORC$	ORC working medium flow	kg/s
n	P&N pair number	pair
p	ORC working medium evaporation pressure	kPa/MPa
q_C	The heat released from the cold end of a thermoelectric power generation sheet	W
q_H	Heat absorbed by the hot end of a thermoelectric power unit	W
Q_C	The heat released from the cold end of the thermoelectric power generation unit	J
Q_H	Heat absorbed by the hot end of the thermoelectric power unit	J
Q_{exh}	Total residual heat when the flue gas temperature drops to 453 K	W
Q_{eva}	Heat absorbed in the evaporator	J
Q_{TEG}/Q_{ORC}	The ratio of TEG bottom cycle to ORC bottom cycle utilization of the waste heat utilization of main engine flue gas	
R_{IN}	Resistance value of a pair of P&N junction	Ω
T_C	Temperature of cold end of thermoelectric power generation unit	K
T_{ORC}	ORC working medium temperature	K
T_H	Hot end temperature of thermoelectric power generation unit	K
t_{op}	Annual operating hours of the system	h
W_{TEG}	Total output power of thermoelectric power generation	W
W_{net}	System net output power	W
Z	Heat exchanger weight or size of equipment power	
z	Annual loan interest rate	
Q_{exh}	Heat release of the condenser	J
W_{exp}	Output power of expander	W
Q_{cond}	Heat release in the condenser	J
$QTEG$	Heat release of thermoelectric power generation unit	J
C_g	System power generation cost	$/kW·h
$CEPCI$	Chemical cost index	
λ_{Cu}	Thermal conductivity of heat source and cold source copper plate	
η_t	System thermal efficiency	
P_{pump}	Working medium pump output power	W
$\eta 1 P_{max}$	thermal efficiency of the TEG bottom cycle	W
P_{min}	the maximum net output power of system	W
	the minimum system output power of system	W